CHEMISTRY OF MATERIALS

ARTICLE

pubs.acs.org/cm

Tuning the Electronic Nature of Aggregation-Induced Emission Luminogens with Enhanced Hole-Transporting Property

Yang Liu,[†] Shuming Chen,[‡] Jacky W. Y. Lam,[†] Ping Lu,[†] Ryan T. K. Kwok,[†] Faisal Mahtab,[†] Hoi Sing Kwok,[‡] and Ben Zhong Tang*[,†,§]

[†]Department of Chemistry and [‡]Center for Display Research, The Hong Kong University of Science & Technology (HKUST), Clear Water Bay, Kowloon, Hong Kong, China

[§]Department of Polymer Science and Engineering, Zhejiang University, Hangzhou 310027, China

Supporting Information

ABSTRACT: Triphenylamine (TPA) is a well-known hole-transporting material but suffers aggregation-caused emission quenching in the solid state. Tetraphenylethene (TPE), on the other hand, is an archetypal luminogen that shows the phenomenon of aggregation-induced emission (AIE). In this work, TPA is attached to the TPE core as peripheral group to generate new AIE luminogens with enhanced hole-transporting property. The TPA-TPE adducts, named 1-[4′-(diphenylamino)biphenyl-4-yl]-1,2,2-triphenylethene (TPATPE) and 1,2-bis[4′-(diphenylamino)biphenyl-4-yl]-1,2-diphenylethene (2TPATPE) are synthesized in satisfactory yields by Suzuki coupling of 4-(diphenylamino)phenylboronic acid with 1-(4-bromophenyl)-1,2,2-triphenylethene and 1,2-bis(4-bromophenyl)-1,2-diphenylethene, respectively. Whereas the hybrid molecules are practically nonluminescent in the solution state, their aggregates in poor solvents and thin films emit intensely with fluorescence quantum yields up to 100%. Both TPATPE and 2TPATPE are thermally and morphologically stable, showing high thermal-degradation (T_d up to 430 °C) and glass transition (T_g = 119 °C) temperatures. Multilayer electroluminescence (EL) devices are constructed, which emit sky blue and green EL with maximum luminance of 32230 cd/m^2 and current efficiency up to 13.0 cd/A. The devices without hole-transporting layers (HTL) show performances comparable to or better than those with HTL, presumably because of the high hole mobility of TPATPE and 2TPATPE coupled with the matching of their energy levels with the anode.

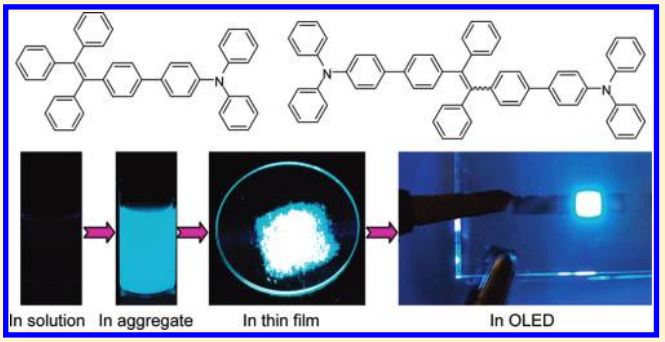

KEYWORDS: fluorescence, tetraphenylethene, triphenylamine, aggregation, hole-transport

INTRODUCTION

Much effort has been devoted to the creation of efficient luminescent materials because of their potential applications in optics and electronics such as electroluminescence (EL), organic lasers, and fluorescent sensors.[1] Whereas many dyes emit strongly in their dilute solutions, they become weak fluorophors when aggregated as nanoparticle suspensions in poor solvents or fabricated as thin films in the condensed phase.[2] This problem must be solved because luminogenic molecules are commonly used as solid films in the real-world applications. Various approaches, such as the attachment of bulky alicyclics, encapsulation by amphiphilic surfactants, and blending with transparent polymers, have been taken to interfere with luminogen aggregation but the attempts have, however, met with only limited success.[3]

We have recently observed "abnormal" emission behaviors of aggregation-induced emission (AIE) and crystallization-enhanced emission. Instead of quenching, aggregate formation of some propeller-shaped molecules such as siloles and tetraphenylethenes (TPEs) has enhanced their light emissions.[4] While crystallization commonly weakens and red-shifts light emission, the crystalline aggregates of some AIE molecules are found to emit stronger, bluer lights than their amorphous counterparts.[5] Organic light-emitting diodes (OLEDs) utilizing the AIE molecules are fabricated, which exhibit outstanding performances.[6]

To enhance the device performance, scientists have fabricated OLEDs with multilayers to balance the charge injection and transportation. In reality, it would be nice to have emitters with both efficient solid-state emissions and good charge-transporting properties because it will simplify the device fabrication procedure, shorten the fabrication process, and lower the production cost.[7] Examples of such fluorophores are tris(8-hydroxyquinolinato)aluminum (Alq_3) and siloles, which are well-known EL emitters and electron-transporting materials.[8] However, AIE luminogens with good hole-transporting properties are rare.

Arylamines such as triphenylamine (TPA) are versatile materials and exhibit good hole-transporting capability.[9] TPA derivatives, however, suffer from the notorious effect of aggregation-caused emission quenching in the condensed phase.[6e] For example, N^4,N^4,

Received: November 30, 2010
Revised: April 14, 2011
Published: April 25, 2011

Chart 1. Chemical Structures of Triphenylamine-Containing Tetraphenylethenes TPATPE and 2TPATPE

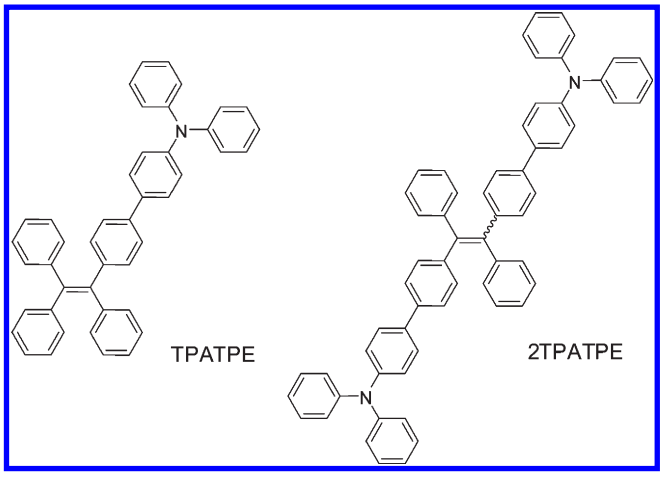

$N^{4'},N^{4'}$-tetraphenylbiphenyl-4,4′-diamine, a TPA dimer, shows a high fluorescence quantum yield (Φ_F) in THF solution (75.6%) but a 5.5-fold lower efficiency in the film state (13.7%). TPE, on the other hand, is AIE-active and enjoys facile synthesis and high thermal stability. Fusing the two components into one system may lead to the generation of new molecules with combined advantages of the two components, that is, both AIE-active and hole-transporting. Intrigued by such possibility, in this paper, we presented the synthesis of TPA-containing tetraphenylethenes (TPATPE and 2TPATPE; Chart 1) and their photophysical properties. Efficient OLEDs using these molecules as both emitters and hole-transporting layers (HTL) are constructed, whose performances are comparable or higher than those with HTL.

EXPERIMENTAL SECTION

Materials and Instrumentations. Tetrahydrofuran (THF) was distilled from sodium benzophenone ketyl under nitrogen immediately prior to use. All the chemicals and other reagents were purchased from Aldrich and used as received without further purification. 4-(Diphenylamino)phenylboronic acid (**1**), 1-(4-bromophenyl)-1,2,2-triphenylethene (BrTPE), and 1,2-bis(4-bromophenyl)-1,2-diphenylethene (2BrTPE) were prepared according to the literature methods.[10,11]

^{1}H and ^{13}C NMR spectra were measured on a Bruker AV 400 spectrometer in $CDCl_3$ or CD_2Cl_2 using tetramethylsilane (TMS; $\delta = 0$) as internal reference. UV spectra were measured on a Milton Roy Spectronic 3000 Array spectrophotometer. Photoluminescence spectra (PL) were recorded on a Perkin-Elmer LS 55 spectrofluorometer. High resolution mass spectra (HRMS) were recorded on a GCT premier CAB048 mass spectrometer operating in MALDI-TOF mode. Thermogravimetric analysis (TGA) was carried on a TA TGA Q5500 under dry nitrogen at a heating rate of 20 °C/min. Thermal transitions were investigated by differential scanning calorimetry (DSC) using a TA DSC Q1000 under dry nitrogen at a heating rate of 10 °C/min. Cyclic voltammograms were recorded on a Princeton Applied Research (model 273A) at room temperature. The working and reference electrodes were glassy carbon and $Ag/AgNO_3$ (0.1 M in acetonitrile), respectively. The HOMO energy levels were derived from the onset oxidation potentials ($E_{onset\text{-}ox}$) according to the equation: HOMO = $-(E_{onset\text{-}ox} + 4.8 - E_{ferrocene})$ eV, where the value of $E_{ferrocene}$ measured in our experiment was 0.11 V. All the solutions were deactivated by bubbling nitrogen gas for a few minutes prior to electrochemical measurements. Transmission electron micrographs and electron diffraction patterns were obtained using JEOL 2010 transmission electron microscope (TEM) at an accelerating voltage of 200 KV. Samples were prepared by casting a drop of suspensions onto copper 400-mesh carrier grids and dried in open air at room temperature.

Device Fabrication. The devices were fabricated on 80 nm ITO-coated glass with a sheet resistance of 25Ω/□. Prior to load into the pretreatment chamber, the ITO-coated glasses were soaked in ultrasonic detergent for 30 min, followed by spraying with deionized water for 10 min, soaking in ultrasonic deionized water for 30 min, and then ovenbake for 1 h. The cleaned samples were treated by CF_4 plasma with a power of 100 W, gas flow of 50 sccm, and pressure of 0.2 Torr for 10 s in the pretreatment chamber. The glasses were transferred to the organic chamber with a base pressure of 7×10^{-7} Torr without breaking vacuum for depositing a 60 nm 4,4-bis(1-naphthylphenylamino)biphenyl (NPB), a 20 nm emitter, a 10 nm 2,2′,2″-(1,3,5-benzinetriyl)tris(1-phenyl-1-*H*-benzimidazole) (TPBi), and a 30 nm Alq_3, which serve as hole-transporting, light-emitting, hole-blocking, and electron-transporting layers, respectively. The samples were then transferred to the metal chamber for cathode deposition which composed of 1 nm LiF capped with 100 nm Al. The light-emitting area was 4 mm^2 defined by the overlap of the cathode and with the anode. The current density−voltage characteristics of the devices were measured on a HP4145B semiconductor parameter analyzer. The forward direction photons emitted from the devices were detected by a calibrated UDT PIN-25D silicon photodiode. The luminance and external quantum efficiencies of the devices were inferred from the photocurrent of the photodiode. The EL spectra were obtained on a PR650 spectrophotometer. All the measurements were carried out under air at room temperature without device encapsulation.

Luminogen Preparation. The TPA-TPE adducts were synthesized according to the synthetic routes shown in Scheme 1. Typical procedures for their syntheses are shown below.

1-[4′-(Diphenylamino)biphenyl-4-yl]-1,2,2-triphenylethene (TPATPE). Into a stirred mixture of 0.411 g (1 mmol) of BrTPE, 0.289 g (1 mmol) of **1**, and 6 mL of 2 M Na_2CO_3 solution in 15 mL THF was added 0.01 g of $Pd(PPh_3)_4$ under nitrogen. The mixture was heated to 80 °C for 12 h. After being cooled to room temperature, the solution was extracted with 50 mL of CH_2Cl_2 twice, washed with water, and dried over Na_2SO_4. After filtration and solvent evaporation under reduced pressure, the product was purified by silica−gel column chromatography using hexane/dichloromethane as eluent. A pale yellow solid was obtained in 66% yield (0.38 g). ^{1}H NMR (400 MHz, $CDCl_3$), δ (TMS, ppm): 7.43−7.45 (m, 2H), 7.32−7.34 (m, 2H), 7.23−7.27 (m, 4H), 7.00−7.13 (m, 25H). ^{13}C NMR (100 MHz, $CDCl_3$), δ (TMS, ppm): 147.67, 147.07, 143.80, 143.77, 143.75, 142.30, 140.98, 140.60, 138.24, 134.60, 131.78, 131.36, 129.24, 127.72, 127.63, 127.47, 126.44, 125.64, 124.32, 123.98, 123.95, 122.86. HRMS (MALDI-TOF): m/z 575.2480 (M^+, calcd 575.2613). Anal. Calcd For $C_{44}H_{33}N$: C, 91.79; H, 5.78; N, 2.43. Found: C, 91.43; H, 5.82; N, 2.45.

1,2-Bis[4′-(diphenylamino)biphenyl-4-yl]-1,2-diphenylethene (2TPATPE). The compound was prepared from 0.4 g (0.6 mmol) of 2BrTPE, 0.416 g (1.44 mmol) of **1**, and 0.02 g of $Pd(PPh_3)_4$ using the same procedure described above. Yellow solid; yield 70% (0.34 g). ^{1}H NMR (400 MHz, $CDCl_3$), δ (TMS, ppm): 7.45 (d, 4H, J = 8.4 Hz), 7.36−7.32 (m, 4H), 7.29−7.23 (m, 8H), 7.15−7.00 (m, 30H). ^{13}C NMR (100 MHz, $CDCl_3$), δ (TMS, ppm): 147.64, 147.05, 143.80, 142.37, 142.35, 140.61, 138.28, 138.20, 134.58, 134.55, 131.79, 131.43, 129.22, 127.75, 127.64, 127.45, 126.47, 126.42, 125.71, 125.61, 124.30, 123.96, 122.84. HRMS (MALDI-TOF): m/z 818.4846 (M^+, calcd 818.3661). Anal. Calcd For $C_{62}H_{46}N_2$: C, 90.92; H, 5.66; N, 3.42. Found: C, 90.53; H, 5.66; N, 3.44.

RESULTS AND DISCUSSIONS

Synthesis. The synthetic routes to the TPA-containing TPEs (TPATPE and 2TPATPE) are depicted in Scheme 1. Compound **1** was synthesized by lithiation of 4-(bromophenyl)diphenylamine followed by boronation with triisopropyl borate.[10] On the other

dx.doi.org/10.1021/cm2003269 |*Chem. Mater.* 2011, 23, 2536–2544

Scheme 1. Synthetic Routes to TPATPE and 2TPATPE

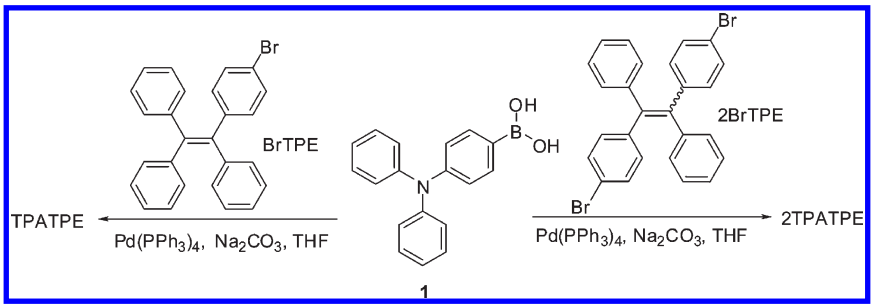

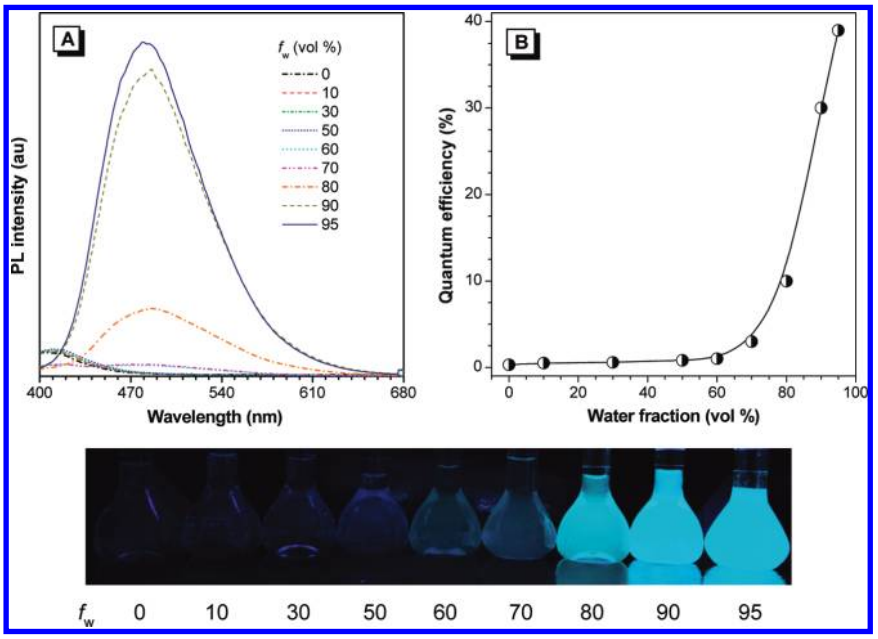

Figure 1. (A) PL spectra of TPATPE in THF/water mixtures with different water fractions (f_w). Concentration, 10 μM; excitation wavelength, 355 nm. (B) Plots of fluorescence quantum yields versus compositions of the THF/water mixtures. Inset: fluorescent images of TPATPE in THF/water mixtures with different water fractions.

hand, the key reactants BrTPE and 2BrTPE were prepared by reaction of diphenylmethyllithium with 4-bromobenzophenone[11a] and McMurry coupling of 4-bromobenzophenone,[11b] respectively. Suzuki coupling reactions[12] of **1** with BrTPE and 2BrTPE are catalyzed by $Pd(PPh_3)_2$ in basic medium, furnishing the desirable products TPATPE and 2TPATPE, respectively, in satisfactory yields (see Experimental Section in the Supporting Information for details). The dye molecules were characterized by NMR spectroscopy and both gave high signal: noise ^{1}H and ^{13}C NMR spectra (see Figures S1−S7 in the Supporting Information). The reaction products, for example, gave M^+ peaks at their high-resolution mass spectra (see Figures S8 and S9 in the Supporting Information), confirming the occurrence of the coupling reaction and the formation of the expected products. The purity of TPATPE and 2TPATPE was also confirmed by elemental analysis with satisfactory results. It is noteworthy that McMurry couplings of monosubstituted benzophenones give TPEs with irregular stereostructures. Intermediate 2BrTPE was prepared from 4-bromobenzophenone using the same reaction. Consequently, the target product 2TPATPE possesses also a low stereoregularity (the zigzag line in the molecular structures of 2BrTPA and 2TPATPE represents that they are mixtures of *Z*- and *E*-isomers). This is proved by the peaks observed at δ 7.6−7.3 in its ^{1}H NMR spectrum (see Figure S3 in the Supporting Information), from which a *Z*/*E* ratio of ~1/1 is deduced. In some occasions, the *Z*- and *E*-isomers can be separated by column chromatography or recrystallization. Unfortunately, these methods are not applicable to 2BrTPE and 2TPATPE because their isomers possess similar polarities. On the other hand, DSC and TGA measurements show that 2TPATPE exhibits only a single glass transition temperature (T_g) and onset degradation temperature (T_d), revealing that the two isomers share similar thermal properties (see Figure 5). Theoretical calculation demonstrates that its *Z*- and *E*-isomers have almost identical orbital distributions and hence exhibit similar fluorescence properties (see Figure 6). All these results make our belief that the existence of both *Z*- and *E*-isomers in 2TPATPE would not alter significantly the overall properties of the material.

Aggregation-Induced Emission. Both TPATPE and 2TPATPE dissolve readily in common organic solvents such as chloroform and THF but are insoluble in water. They are practically nonemissive when molecularly dissolved in the solutions but emit intensely in the aggregate state. As shown in Figures 1 and 2, the PL

dx.doi.org/10.1021/cm2003269 |*Chem. Mater.* 2011, 23, 2536–2544

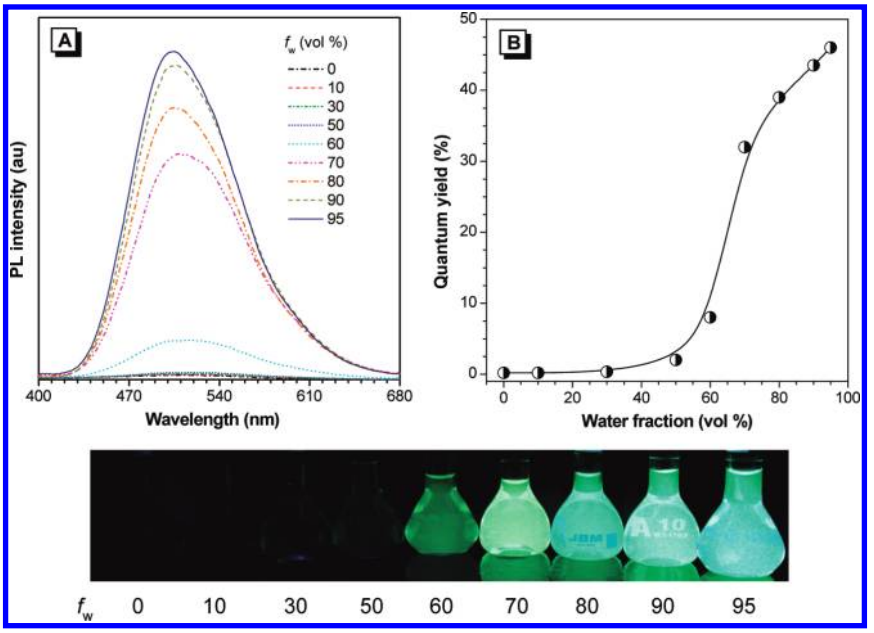

Figure 2. (A) PL spectra of 2TPATPE in THF/water mixtures with different water fractions (f_w). Concentration, 10 μM; excitation wavelength, 355 nm. (B) Plots of fluorescence quantum yields versus the compositions of the THF/water mixtures. Inset: fluorescent images of 2TPATPE in THF/water mixtures with different water fractions.

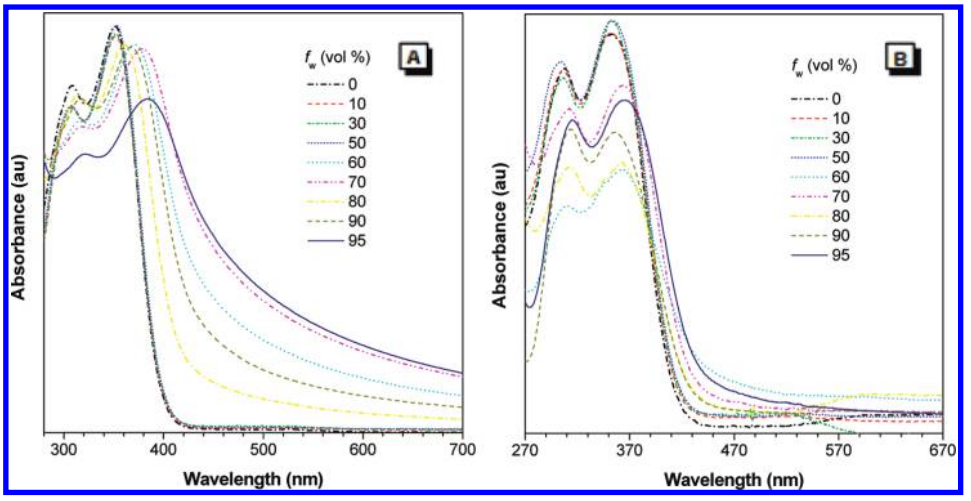

Figure 3. UV spectra of (A) TPATPE and (B) 2TPATPE in THF/water mixtures with different water fractions (f_w).

spectra of TPATPE and 2TPATPE in THF are basically flat lines parallel to the abscissa. The Φ_F's in THF are as low as 0.38 and 0.24%, respectively, revealing that TPATPE and 2TPATPE are genuinely weak emitters in the solution state. When a large amount of water is added into their THF solutions, intense PL signals are recorded at 480 and 505 nm under identical measurement conditions. The higher the water fraction, the stronger is the emission intensity. Since water is a nonsolvent for TPATPE and 2TPATPE, their molecules must be aggregated in the solvent mixtures with high water fractions. From the molecular solution in THF to the aggregate suspension in 95% aqueous mixture, the Φ_F's of TPATPE and 2TPATPE increase ca. 103- and 192-fold, respectively. Apparently, their emissions are induced by aggregate formation; in other words, they are AIE-active. The aqueous mixtures are, however, macroscopically homogeneous with no precipitates, suggesting that the aggregates are of nanodimension, as proved by the level-off tails at the longer wavelength region of their absorption spectra in the aqueous mixtures with high water contents due to the scattering effect of the dye nanoparticles (Figure 3). The photographs in the lower panels of Figures 1 and 2 further manifest the nonluminescent and emissive natures of the molecular isolated species and nanoaggregates.

Closer inspection of the PL spectra of the two compounds in the aqueous mixtures reveals that the emission maximum is blue-shifted slightly when the water fraction is increased from 70 to 95%. This is probably due to the change in the packing order of the aggregates from an amorphous state to a crystalline one.[13] This is proved by the TEM images and the electron diffraction patterns in Figure 4. Whereas the aggregates formed in the solvent mixtures with 90% water fractions display many clear diffraction spots, those derived from 70% aqueous mixtures give only an obscure diffuse halo, suggesting that they are crystalline

and amorphous in nature, respectively (see Figure S10 in the Supporting Information).

Like their aggregates suspended in the aqueous media, TPATPE and 2TPATPE are highly emissive in the solid state. Upon photoexcitation, their thin films emit at 486 and 505 nm with Φ_F values of 100% (Table 1), which are more than 2-fold higher than that of unsubstituted TPE (49.2%).[14]

It is worth mentioning that TPA is emissive in solution.[6e] The nonluminescent nature of TPATPE and 2TPATPE in the solution state suggests that the TPE core quenches the light emission. In solution, the active intramolecular rotations of the phenyl blades around the TPE stator may have effectively deactivated the excited states via the rotational energy relaxation channels, thus rendering TPATPE and 2TPATPE nonemissive. In the aggregate state, the intramolecular rotations are restricted,

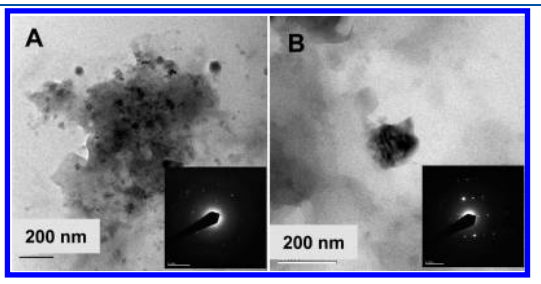

Figure 4. TEM images of nanoaggregates of (A) TPATPE and (B) 2TPATPE formed in THF/water mixtures with 95% water fractions. Insets: electron diffraction patterns of the nanoaggregates.

Table 1. Optical and Thermal Properties of TPATPE and 2TPATPE[a]

	λ_{em} (nm)				
AIE luminogen	soln (Φ_F)	aggr (Φ_F)	film (Φ_F)	T_d (°C)	T_g (°C)
TPATPE	405 (0.38)	480 (39)	486 (100)	360	
2TPATPE	511 (0.24)	505 (46)	505 (100)	430	119

[a] Abbreviations: λ_{em} = emission maximum in THF solutions (soln; 10 μM), THF/water mixtures (aggr; 10 μM; 5:95 by volume), and solid thin films with quantum yields (Φ_F, %) given in the parentheses, T_d = onset degradation temperature, and T_g = glass transition temperature. The Φ_F values in the solution and aggregate states were determined by using quinine sulfate (Φ_F = 54% in 0.1 M sulphuric acid as standard, whereas that of solid film was measured using a calibrated integrating sphere.

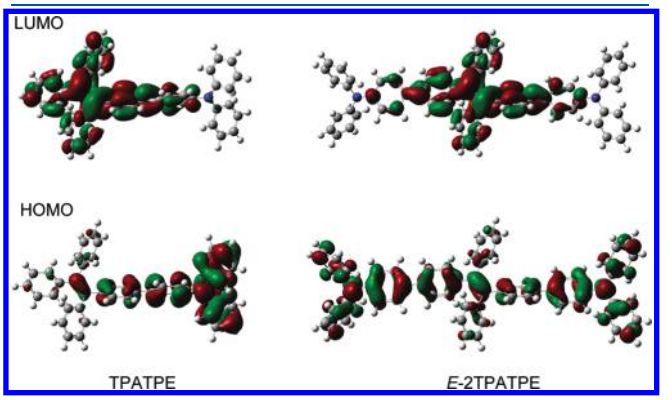

Figure 6. Optimized geometries and molecular orbital amplitude plots of HOMO and LUMO energy levels of TPATPE and *E*-2TPATPE.

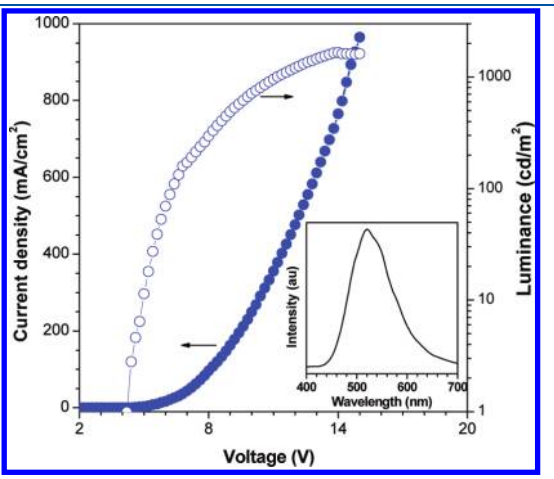

Figure 7. Changes in current and luminance with the applied voltage in a single-layer EL device of 2TPATPE with a configuration of ITO/2TPATPE/LiF/Al. Inset: EL spectrum of the device.

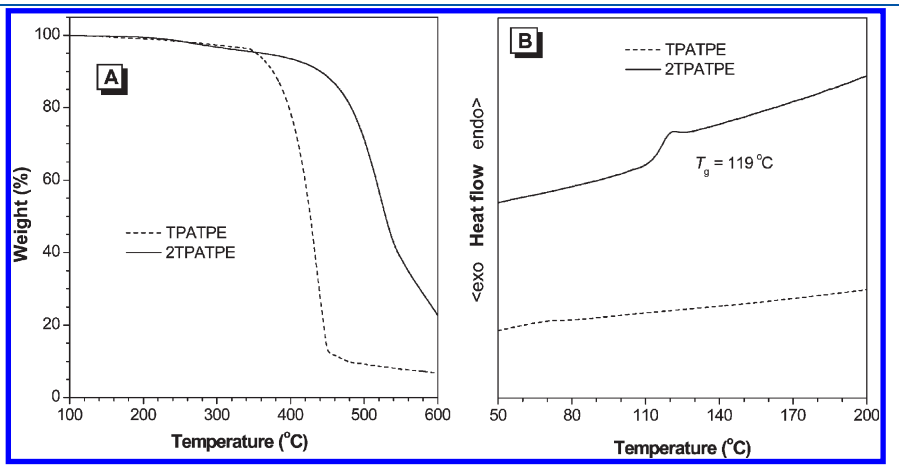

Figure 5. (A) TGA and (B) DSC (second heating cycle) thermograms of TPATPE and 2TPATPE recorded under N_2 at a heating rate of (A) 20 and (B) 10 °C/min.

dx.doi.org/10.1021/cm2003269 |*Chem. Mater.* 2011, 23, 2536–2544

which block the nonradiative pathways and populate the radiative decay. On the other hand, the propeller-like TPE unit would efficiently hamper the close packing between the chromophores, preventing the formation of detrimental species such as excimers and exciplexes that cause emission quenching and red-shift in the PL spectrum. All these factors have converted TPATPE and 2TPATPE from weak fluorophors into strong emitters.

Thermal Properties. The thermal properties of TPATPE and 2TPATPE are investigated by TGA and DSC analyses. As shown in Figure 5A, both TPATPE and 2TPATPE enjoy high thermal stability with T_d's of 360 and 430 °C, respectively, which are much higher than that of TPE (T_d = 224 °C).[14d] DSC analysis of 2TPATPE during the second heating cycle detects a T_g at 119 °C, which is higher than that of NPB (T_g = 96 °C). This suggests that 2TPATPE possesses a high morphological stability. Coupled with its efficient solid-state emission, the dye is thus a promising EL material. The T_g of TPATPE is not detected, probably because of its low molecular weight.

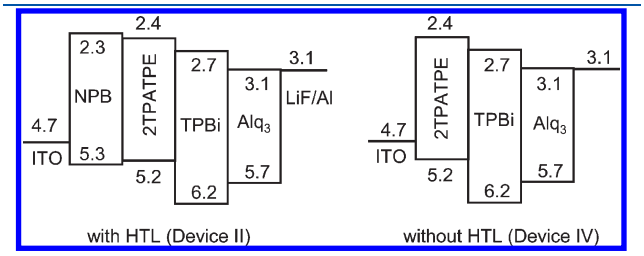

Figure 8. Energy level diagrams and device configurations of multilayer EL devices of 2TPATPE with and without NPB or hole-transporting layers. Abbreviations: NPB = 4,4-bis(1-naphthylphenylamino)biphenyl, TPBi = 2,2′,2″-(1,3,5-benzinetriyl)tris(1-phenyl-1-*H*-benzimidazole).

Electronic Structure. To better understand the photophysical properties of TPATPE and 2TPATPE, we performed molecular calculations on their energy levels based on DFT/B3LYP/6-31G(d) using Gaussian 03. The optimized geometries and HOMO and LUMO plots of TPATPE and *E*-2TPATPE are given in Figure 6. Both molecules adopt twisted conformations, whose geometries are similar to the crystal structure of TPE.[15] The dihedral angles between any two phenyl rings of the TPE core are in the range from 58 to 80°. Such propeller-like, nonplanar conformations would hamper the $\pi-\pi$ stacking interactions between the dye molecules, which enable them to emit efficiently in the condensed phase. The dihedral angle between the adjacent phenyl blades of the TPE and TPA units is ~36°, which makes the two chromophores moderate conjugated. The LUMO of both molecules are dominated by orbitals from the TPE core. In contrast, the electron cloud of the HOMO is located mainly on the TPA unit. Such electron distribution imparts the dye molecules with an intrinsic intramolecular charge transfer property. The molecular orbitals are more "delocalized" in *E*-2TPATPE, suggesting that it possesses a higher conjugation and thus shows a redder

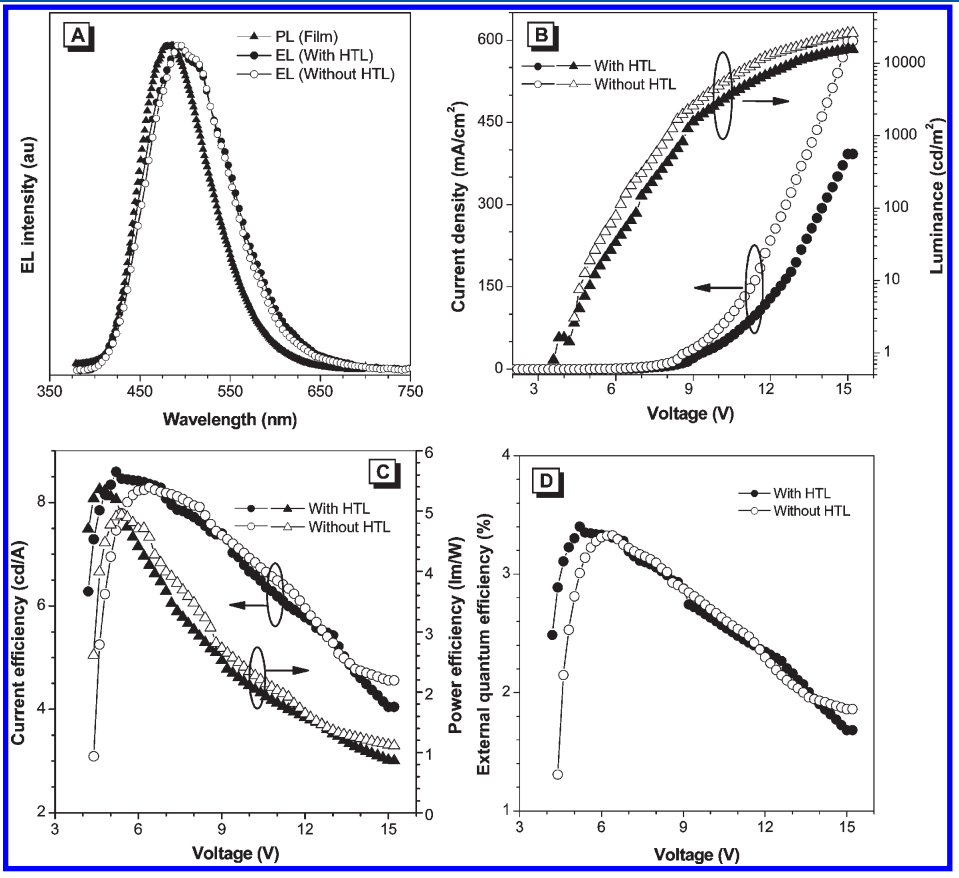

Figure 9. (A) PL and EL spectra of solid thin film of TPATPE. (B) Current density−voltage−luminance characteristics of multilayer EL devices of TPATPE. Changes in (C) power and current and (D) external quantum efficiencies with the applied voltage in multilayer EL devices of TPATPE. Device configurations: ITO/(HTL)/TPATPE/TPBi/Alq_3/LiF/Al.

dx.doi.org/10.1021/cm2003269 |*Chem. Mater.* 2011, 23, 2536–2544

Table 2. Electroluminescence Performances of TPATPE and 2TPATPE[a]

device	LEL	HTL	λ_{EL} (nm)	V_{on} (V)	L_{max} (cd/m^2)	CE_{max} (cd/A)	PE_{max} (lm/W)	EQE_{max} (%)
I	TPATPE	√	492	3.6	15480 (15 V)	8.6 (5.2 V)	5.3 (4.6 V)	3.4 (5.2 V)
III		×	492	4.2	26090 (15 V)	8.3 (6.4 V)	4.9 (5.4 V)	3.3 (6.0 V)
II	2TPATPE	√	514	3.4	32230 (15 V)	12.3 (4.2 V)	10.1 (3.8 V)	4.0 (4.2 V)
IV		×	512	3.2	33770 (15 V)	13.0 (4.2 V)	11.0 (3.6 V)	4.4 (4.2 V)

[a] With device configurations of ITO/(HTL)/LEL/TPBi/Alq_3/LiF/Al. Abbreviations: LEL = light-emitting layer, HTL = hole-transporting layer, λ_{EL} = EL maximum, V_{on} = turn-on voltage at 1 cd m^{-2}, L_{max} = maximum luminance, CE_{max} = maximum current efficiency, PE_{max} = maximum power efficiency, and EQE_{max} = maximum external quantum efficiency.

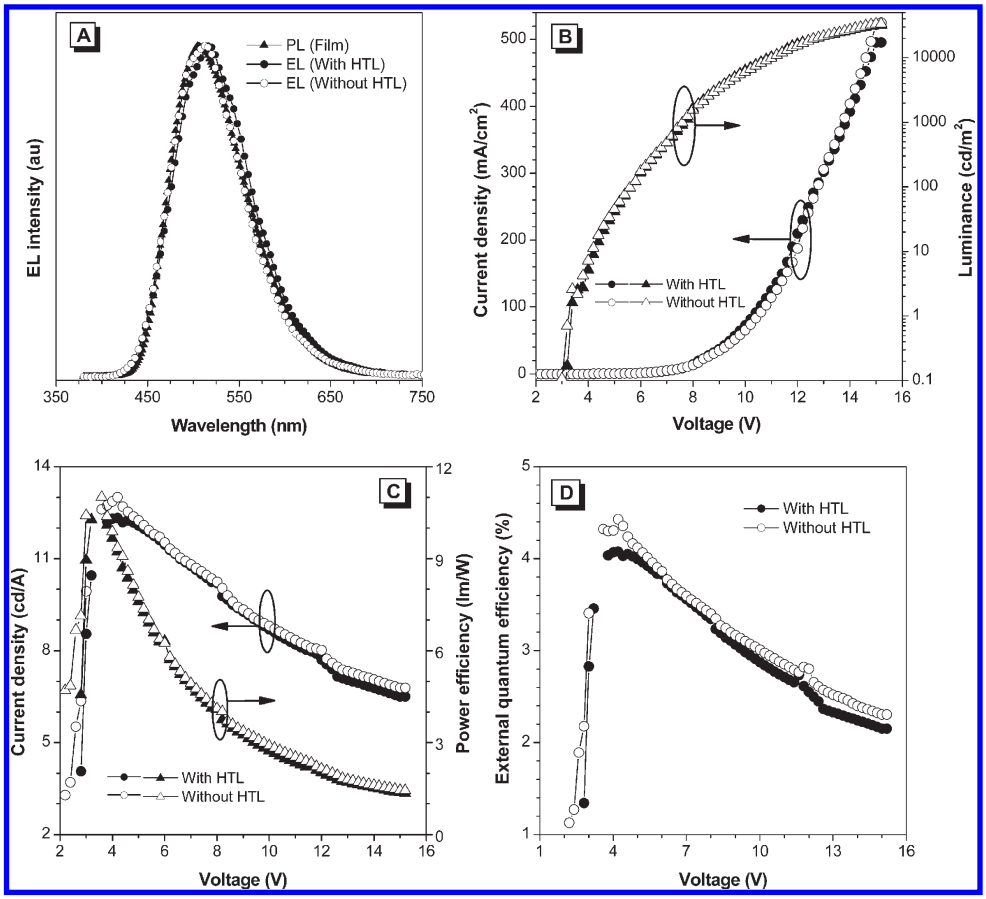

Figure 10. (A) PL and EL spectra of solid thin film of 2TPATPE. (B) Current density−voltage−luminance characteristics of multilayer EL devices of 2TPATPE. Changes in (C) power and current and (D) external quantum efficiencies with the applied voltage in multilayer EL devices of 2TPATPE. Device configurations: ITO/(HTL)/2TPATPE/TPBi/Alq_3/LiF/Al.

emission than TPATPE. Similar orbital distribution is also observed in *Z*-2TPATPE.

The electrochemical properties of TPATPE and 2TPATPE are investigated by cyclic voltammetry. Such method is also widely used for estimating the energy levels of organic semiconductors. Both dye molecules exhibit similar voltammograms (see Figure S11 in the Supporting Information). Their HOMO derived from the onset oxidation potentials are calculated to be 5.3 and 5.2 eV, respectively, which are the same to or slightly higher than that of NPB. Their LUMO are obtained by subtraction of the optical band gap energies from the HOMO values and are both equal to 2.4 eV.

Electroluminescence. The efficient light emissions of TPATPE and 2TPATPE in the solid state prompt us to investigate their EL properties. We first constructed a single-layer EL device with a configuration of ITO/2TPATPE(100 nm)/LiF/Al(200 nm) using 2TPATPE as light-emitting layer (LEL). Figure 7 shows the *J*−*V*−*L* characteristics of the device. The device emits at 518 nm, exhibiting maximum luminance (L_{max}) and current and power efficiencies (CE_{max} and PE_{max}) of 1630 cd/m^2, 0.43 cd/A, and 0.22 lm/W, respectively. Although the result is fair, it already demonstrates that 2TPATPE possesses good charge-injecting and transporting properties.

To enhance the device performance, multilayer OLEDs with a configuration of ITO/NPB(40 nm)/LEL(20 nm)/TPBi(10 nm)/Alq_3(30 nm)/LiF/Al(200 nm) (for device I, LEL = TPATPE; for device II, LEL = 2TPATPE) are fabricated, in which NPB functions as HTL and TPBi and Alq_3 serve as electron-transporting materials. Since the result from Figure 7 reveals that TPATPE and 2TPATPE may retain the good hole-transporting properties of their TPA

dx.doi.org/10.1021/cm2003269 |*Chem. Mater.* 2011, 23, 2536–2544

peripheries, the use of NPB as an additional HTL is thus not necessary and could be even harmful because it may break the charge balance in the EL device. With such regard, we fabricated devices III and IV, in which the NPB or hole-transporting layers in devices I and II are eliminated. The energy level diagrams and the device architectures of 2TPATPE are depicted in Figure 8 as example.

The EL spectra of both devices of TPATPE peak at 492 nm, which is similar to the PL peak of the thin film (Figure 9A). The EL performance of device I is impressive, with CE_{max}, PE_{max}, and external quantum efficiency (EQE_{max}) being 8.6 cd/A, 5.3 lm/W, and 3.4%, respectively (Table 2). Similar outstanding data (8.3 cd/A, 4.9 lm/W, and 3.3%) are also achieved in device III. At the same voltage, device III shows better electronic character and radiates more intensely than device I (Figure 9B). Clearly, TPATPE is an excellent hole-transporting material, in addition to being highly emissive in the solid state.

The OLED fabricated from 2TPATPE without a NPD layer (device IV) shows even better performance. The device turns on at a low bias of 3.2 V, emitting brilliantly with maximum luminance of 33770 cd/m^2 (Figure 10). The CE_{max} and PE_{max} reach 13.0 cd/A and 11.0 lm/W, which are higher than those attained by device II (Table 2). The high hole mobility of 2TPATPE and its matched HOMO energy level with the anode may enable it to exhibit better EL performance in the absence of NPB. The EQE_{max} is 4.4% and is comparable or even better than most of the results reported previously for singlet OLEDs.[6g] One thing that needs to be pointed out is that with a similar device structure, the unsubstituted TPE only shows L_{max} and CE_{max} of 1800 cd/m^2 and 0.45 cd/A.[15] Apparently, the EL properties of TPE can be readily tuned by molecular engineering endeavors and incorporation of TPA as substituent to TPE has resulted in new AIE luminogens with higher thermal stability, more efficient solid-state emissions, and enhanced hole-transporting properties. All these attributes make TPATPE and 2TPATPE better EL materials for OLED application.

CONCLUSIONS

In this paper, TPA-containing tetraphenylethenes TPATPE and 2TPATPE are synthesized and their optical properties are investigated. Whereas they are almost nonluminescent when molecularly dissolved in the solutions, they are induced to emit intensely by aggregate formation, demonstrating an AIE phenomenon. The AIE effect has boosted the quantum yields of their solid thin films to unity. Both dye molecules enjoy high thermal stability (≥360 °C) and are morphological stable. Multilayer EL devices with configurations of ITO/(NPB)/TPATPE or 2TPATPE/TPBi/Alq_3/LiF/Al are constructed, which give sky blue and green EL with maximum luminance and efficiencies of 33700 cd/m^2, 13.0 cd/A, 11.0 lm/W, and 4.4%. The OLEDs without hole-transporting layers show comparable or better performances than those with HTL, possibly to the high hole mobility of the TPA unit in the hybrid molecules.

The present results demonstrate that combining ACQ and AIE units in one molecule is a good approach to surmount the notorious ACQ problem. Traditional approaches attempt to prevent luminophors from forming aggregates but generate new problems. Our strategy, however, takes advantage of chromophore aggregation without sacrificing other functional properties of the luminophors. Through such a tool, it is anticipated that new AIE luminogens with new and/or enhanced functional properties will be generated.

ASSOCIATED CONTENT

Supporting Information. ^{1}H and ^{13}C NMR spectra, UV absorption spectra, TEM images of nanoaggregates, and CV spectra of TPATPE and 2TPATPE. This material is available free of charge via the Internet at http://pubs.acs.org.

AUTHOR INFORMATION

Corresponding Author

*E-mail: tangbenz@ust.hk. Phone: +852-2358-7375. Fax: +852-2358-1594.

ACKNOWLEDGMENT

This project was partially supported by the Research Grants Council of Hong Kong (603509, 601608, CUHK2/CRF/08, and HKUST2/CRF/10), the Innovation and Technology Commission (ITP/008/09NP and ITS/168/09), the University Grants Committee of Hong Kong (AoE/P-03/08), and the National Science Foundation of China (20974028). B.Z.T. thanks the support from Cao Guangbiao Foundation of Zhejiang University.

REFERENCES

(1) (a) Tang, C. W.; VanSlyke, S. A. *Appl. Phys. Lett.* **1987**, *51*, 913. (b) Mullen, K.; Scherf, U. *Organic Light-Emitting Devices. Synthesis, Properties and Applications*; Wiley: Weinheim, Germany, 2006. (c) Roncali, J.; Leriche, P.; Cravino, A. *Adv. Mater.* **2007**, *19*, 2045. (d) Liu, B.; Dan, T. T. T.; Bazan, G. C. *Adv. Funct. Mater.* **2007**, *17*, 2432. (e) Yang, S. H.; Hsu, C. S. *J. Polym. Sci., Part A: Polym. Chem.* **2008**, *46*, 7173.

(2) (a) Grimsdale, A. C.; Chan, K. L.; Martin, R. E.; Jokisz, P. G.; Holmes, A. B. *Chem. Rev.* **2009**, *109*, 897. (b) Shimizu, M.; Tatsumi, H.; Mochida, K.; Shimono, K.; Hiyama, T. *Chem. Asian J.* **2009**, *4*, 1289. (c) Pu, K. Y.; Liu, B. *Adv. Funct. Mater.* **2009**, *19*, 277. (d) Iida, A.; Yamaguchi, S. *Chem. Commun.* **2009**, 3002. (e) Saragi, T. P. I.; Spehr, T.; Siebert, A.; Fuhrmann-Lieker, T.; Salbeck, J. *Chem. Rev.* **2007**, *107*, 101. (f) Yin, S.; Peng, Q.; Shuai, Z.; Fang, W.; Wang, Y.; Luo, Y. *Phys. Rev. B* **2006**, *73*, 205409. (g) Kawamura, Y.; Goushi, K.; Brooks, J.; Brown, J. J.; Sasabe, H.; Adachi, C. *Appl. Phys. Lett.* **2005**, *86*, 071104. (h) Koren, A. B.; Curtis, M. D.; Francis, A. H.; Kampf, J. W. *J. Am. Chem. Soc.* **2003**, *125*, 5040. (i) Destri, S.; Pasini, M.; Botta, C.; Porzio, W.; Bertini, F.; Marchio, L. *J. Mater. Chem.* **2002**, *12*, 924. (j) An, B.-K.; Kwon, S.-K.; Jung, S.-D.; Park, S. Y. *J. Am. Chem. Soc.* **2002**, *124*, 14410. (k) Friend, R. H.; Gymer, R. W.; Holmes, A. B.; Burroughes, J. H.; Marks, R. N.; Taliani, C.; Bradley, D. D. C.; Dos Santos, D. A.; Brédas, J. L.; Lögdlund, M.; Salaneck, W. R. *Nature* **1999**, *397*, 121. (l) Baldo, M. A.; O'Brien, D. F.; You, Y.; Shoustikov, A.; Sibley, S.; Thompson, M. E.; Forrest, S. R. *Nature* **1998**, *395*, 151.

(3) (a) Lee, S. H.; Jang, B. B.; Kafafi, Z. H. *J. Am. Chem. Soc.* **2005**, *127*, 9071. (b) Marsitzky, D.; Vestberg, R.; Blainey, P.; Tang, B. T.; Hawker, C. J.; Carter, K. R. *J. Am. Chem. Soc.* **2001**, *123*, 6965. (c) Setayesh, S.; Grimsdale, A. C.; Weil, T.; Enkelmann, V.; Muellen, K.; Meghdadi, F.; List, E. J. W.; Leising, G. *J. Am. Chem. Soc.* **2001**, *123*, 946.

(4) (a) Luo, J.; Xie, Z.; Lam, J. W. Y.; Cheng, L.; Chen, H.; Qiu, C.; Kwok, H. S.; Zhan, X.; Liu, Y.; Zhu, D.; Tang, B. Z. *Chem. Commun.* **2001**, 1740. (b) Hong, Y.; Lam, J. W. Y.; Tang, B. Z. *Chem. Commun.* **2009**, 4332. (c) Liu, J.; Lam, J. W. Y.; Tang, B. Z. *J. Inorg. Organomet. Polym. Mater.* **2009**, *19*, 249. (d) Tang, B. Z. *Macromol. Chem. Phys.* **2009**, *210*, 900.

(5) Dong, Y.; Lam, J. W. Y.; Qin, A.; Sun, J.; Liu, J.; Li, Z.; Sun, J.; Sung, H. H. Y.; Williams, I. D.; Kwok, H. S.; Tang, B. Z. *Chem. Commun.* **2007**, 40.

(6) (a) Chen, H.; Lam, W. Y.; Luo, J.; Ho, Y.; Tang, B. Z.; Zhu, D.; Wong, M.; Kwok, H. S. *Appl. Phys. Lett.* **2002**, *81*, 574. (b) Liu, Y.; Tao, X.;

Wang, F.; Shi, J.; Yu, W.; Ren, Y.; Zou, D.; Jiang, M. *J. Phys. Chem. C* **2007**, *111*, 6544. (c) Liu, Y.; Tao, X.; Wang, F.; Dang, X.; Zou, D.; Ren, Y.; Jiang, M. *J. Phys. Chem. C* **2008**, *112*, 3975. (d) Ning, Z.; Chen, Z.; Zhang, Q.; Yan, Y.; Qian, S.; Cao, Y.; Tian, H. *Adv. Funct. Mater.* **2007**, *17*, 3799. (e) Yuan, W. Z.; Lu, P.; Chen, S.; Lam, J. W. Y.; Wang, Z.; Liu, Y.; Kowk, H. S.; Ma, Y.; Tang, B. Z. *Adv. Mater.* **2010**, *22*, 2159. (f) Zhao, Z.; Chen, S.; Shen, X.; Mahtab, F.; Yu, Y.; Lu, P.; Lam, J. W. Y.; Kwok, H. S.; Tang, B. Z. *Chem. Commun.* **2010**, *46*, 686. (g) Zhao, Z.; Chen, S.; Lam, J. W. Y.; Lu, P.; Zhong, Y.; Wong, K. S.; Kwok, H. S.; Tang, B. Z. *Chem. Commun.* **2010**, *46*, 2221.

(7) Tao, S.; Li, L.; Yu, J.; Jiang, Y.; Zhou, Y.; Lee, C. S.; Lee, S. T.; Zhang, X.; Kwon, O. *Chem. Mater.* **2009**, *21*, 1284.

(8) Yu, G.; Yin, S.; Liu, Y.; Chen, J.; Xu, X.; Sun, X.; Ma, D.; Zhan, X.; Peng, Q.; Shuai, Z.; Tang, B. Z.; Zhu, D.; Fang, W.; Luo, Y. *J. Am. Chem. Soc.* **2005**, *127*, 6335.

(9) (a) Mikroyannidisa, J. A.; Tsai, L.-R.; Chen, Y. *Synth. Met.* **2009**, *159*, 78. (b) Shirota, Y. *J. Mater. Chem.* **2000**, *10*, 1. (c) Moorthy, J. N.; Venkatakrishnan, P.; Huang, D.-F.; Chow, T. J. *Chem. Commun.* **2008**, 2146.

(10) Banerjee, M.; Edmond, S. J.; Lindeman, S. V.; Rathore, R. *J. Org. Chem.* **2007**, *72*, 8054.

(11) (a) Sun, M.; Li, J.; Li, B.; Fu, Y.; Bo, Z. *Macromolecules* **2005**, *38*, 2651. (b) McMurry, J. E. *Chem. Rev.* **1989**, *89*, 1513.

(12) Miyaura, N.; Suzuki, A. *Chem. Rev.* **1995**, *95*, 2457.

(13) Zhu, L.; Yang, C.; Qin, J. *Chem. Commun.* **2008**, 6303.

(14) (a) Tong, H.; Hong, Y.; Dong, Y.; Haussler, M.; Lam, J. W. Y.; Li, Z.; Guo, Z.; Guo, Z. H.; Tang, B. Z. *Chem. Commun.* **2006**, 3705. (b) Sung, H. H. Y.; Williams, I. D.; Tang, B. Z. *J. Phys. Chem. B* **2007**, *111*, 11817. (c) Hong, Y.; Häussler, M.; Lam, J. W. Y.; Li, Z.; Sin, K.; Dong, Y.; Tong, H.; Liu, J.; Qin, A.; Renneberg, R.; Tang, B. Z. *Chem.—Eur. J.* **2008**, *14*, 6428. (d) Zhao, Z.; Chen, S.; Lam, J. W. Y.; Jim, C. K. W.; Chan, C. Y. K.; Wang, Z.; Lu, P.; Deng, C.; Kwok, H. S.; Ma, Y.; Tang, B. Z. *J. Phys. Chem.* **2010**, *114*, 7963.

(15) Dong, Y.; Lam, J. W. Y.; Qin, A.; Liu, J.; Li, Z.; Tang, B. Z. *Appl. Phys. Lett.* **2007**, *91*, 011111.